Strength Analysis of the Main Structural Component in Ship-to-Shore Cranes Under Dynamic Load

Gang Tang, Chen Shi, Yide Wang, Xiong Hu

Strength analysis of the main structural component in ship-to-shore cranes under dynamic load

GANG TANG[1,2], CHEN SHI[1,2],YIDE WANG[2] and XIONG HU[1]
[1]Logistics Engineering College, Shanghai Maritime University, Shanghai 201306, China
[2]Université de Nantes IETR, Nantes, UMR CNRS 6164 , France

Corresponding author: Xiong Hu (e-mail:huxiong@shmtu.edu.cn); Chen Shi(e-mail:shichen77@qq.com)

ABSTRACT After a period of operation, the mechanical properties of ship-to-shore (STS) cranes can change. It is necessary to analyze the strength of the main structural component in STS cranes under dynamic load to assess their safety. This case study was conducted on a 28-ton capacity STS crane. A testing system with signal sensing, conditioning, acquiring, and analysis was established. After on-site testing, all of the stresses of the test positions were calculated and determined to be in the allowable range. As a result of this study, a systematic approach to analyze the strength of the main structural component in STS cranes under dynamic load is proposed.

INDEX TERMS ship-to-shore cranes, dynamic load, Kalman filters

I. INTRODUCTION

SHIP-to-shore (STS) cranes are used in ports and terminals to transfer containerized cargo to and from ships [1]. Since its inception more than 50 years ago (the first quayside container crane was built in January 1959 [2]), the container industry has made remarkable progress. The typical elements of an STS crane include a combination of two sets of ten rail wheels mounted to the bottom of the vertical frame and braced system; a structurally designed system of beams assembled to support the boom, cabin, operating machinery, and the cargo being lifted; crane boom; hook; operating cabin; and storage equipment. The crane is driven by a specially trained operator who sits in a cabin attached to the trolley suspended from the beam. The trolley runs along rails located on the top or sides of the boom and girder. The operator runs the trolley over the ship to lift the cargo, usually containers. Once the spreader locks onto the container, the container is lifted, moved over the dock, and placed on a truck chassis (trailer) to be taken to the storage yard. The crane also lifts containers from the chassis on the dock to load them onto the ship.

STS cranes are mostly used for a long duration. Prolonged use affects the mechanical properties of STS cranes. If an accident occurs, the economic losses can be enormous, and thus, safety assessments are necessary. There are many performance indicators related to STS crane safety, including structure strength, dynamic stiffness, and fatigue strength. The main objective of this paper is to study the strength of the main structural component in STS cranes under dynamic load.

There are many studies on machines under dynamic load. For example, a simple experimental technique employing wire strain gauges for measuring dynamic loads and stresses in operating gear systems has been described in [3]. Others have applied simple rigid-plastic methods to analyze plastic failure of ductile beams loaded dynamically, as N Jones in [4]. JA Laman et al. [5] have calculated the dynamic load allowance in steel through-truss bridges. PS Shenoy et al. [6] have performed quasi-dynamic finite element analysis (FEA) for a typical connecting rod to capture stress variations over a cycle of operation. ES Hwang et al. [7] have analyzed the simulation of dynamic loads in bridges. VA Kopnov [8] has predicted the fatigue life of the metalwork of a travelling gantry crane. Some experiments on a welded steel frame exposed to fatigue loading, and on wire ropes damaged by saw cuts have been conducted in [9]. Research about the sensitivity of some sources of uncertainty in the seismic response of a Korean container crane structure has been reported in [10]. A comparative study of nonlinear static and time history analyses of typical Korean STS container cranes has been described in [11]. Furthermore, there are some published books about the impact strength of materials [12] and introductions to examples of structural computation of machine components [13]. However, in the existing litera-

ture, we have not found a systematic testing approach applied to STS cranes under dynamic load. However, all the previous studies lack of systematic approach in analyzing the strength of the main structure component in STS crane under dynamic load.

In this paper, the dynamic load strength test is designed to determine whether the main structural component of an STS crane can withstand transient impact stresses caused by preset loads and changes in the trolley position. Simulating the worst working conditions allow us to determine whether the structure meets strength requirements. In this paper, a study on an STS crane with 28-ton capacity and 18 years of service has been conducted with on-site testing. We have not conduct field tests under strong wind conditions because of the safety concerns [14].

The remainder of the paper is organized as follows. In section II, we introduce the test method, including the principles of the testing system, the location of measuring points to find the loading, and the conditions. In section III, we summarize the data and analyze it with Kalman filters, showing the maximum value of stress at each measuring point. In section IV, we present our conclusions.

II. TESTING METHOD

A. TESTING SYSTEM

The dynamic load test assesses the dynamic loading stresses in the main girder carrying the member system, rod system, and gantry system. Tensile stress is expressed as positive while compressive stress is negative. Figure 1 shows a schematic structure of our dynamic load strength test and analysis. It includes strain measuring points, signal sensing and conditioning, signal analysis, and output. The signals enter a 14-channel strain gauge signal conditioner to be processed and amplified. One of the advantages of this testing system is that it can produce a stable gauge output signal. Using the on-site data acquisition system, the parameters of the dynamic load working condition can be obtained. These data and synchronously processed signals will be stored in the specified virtual instrument memory for the secondary processing.

Dynamic load stress testing and analysis of the main equipment will use the following instruments and sensors:

1) electrical resistance strain gauges,
2) quad strain adapter, and
3) crane status monitoring and evaluation system, which mainly includes
   a) workstation,
   b) signal channel expansion box,
   c) signal conditioning apparatus,
   d) data collector,
   e) visualization software, and
   f) data management and analysis software.

B. MEASURING POINTS

The beam of an STS crane is primarily subjected to transverse and axial loads. When we analyze the strength of the main structural component, we ignore axial loads. Consider a beam that is simply-supported at E and K, and subjected to three concentrated loads and two distributed loads as shown in Figure 2. F_x is the dynamic load acting on the beam; the location of X can be changed along the beam. The transverse loads cause internal shear forces and bending moments, which in turn cause axial stresses and shear stresses in the cross section. Considering the reactions as plane stress states, we obtain the following empirical equation for calculating the total stress [15]:

$$\sigma = \sqrt{\sigma_1^2 + \sigma_m^2 - \sigma_1\sigma_m + 3\tau^2} \tag{1}$$

where σ_1 is the longitudinal axial stress caused by the bending moment, σ_m is the compressive stress caused by the concentrated load, and τ is the shear stress. The simple theory of elastic bending states that

$$\sigma_1 = \frac{M_{max}}{Z} \tag{2}$$

where M_{max} is the maximum bending moment for the beam and Z is the section modulus. If the force is evenly distributed across the cross section, the internal forces can be approximated as uniform, and the beam is subjected to a uniform normal stress, defined as

$$\sigma_m = \frac{P}{\delta C} \tag{3}$$

with P the concentrated load, δ the width (depth) of the concentrated load, and C the length of the concentrated load.

When the beam is subjected to a set of equal and opposite transverse forces, there is a tendency to failure caused by stratification of the material. If this failure is restricted, then a shear stress τ is generated, defined as

$$\tau = \frac{QA_r}{I\sum\delta} \tag{4}$$

with I the moment of inertia, Q the shear force, A_r the area of the cross section, and $\sum$ the summation. To calculate these parameters, it is necessary to analyze the cross section of the beam, which is a rectangular tube, as shown in Figure 3. Assuming that the beam is symmetric about the neutral axis passing through its centroid, we can calculate the relevant geometric parameters as

$$\begin{cases} A_r = ab - a_1b_1 \\ I = \dfrac{ab^3 - a_1b_1^3}{12} \\ Z = \dfrac{ab^3 - a_1b_1^3}{6b} \\ e = \dfrac{b}{2} \\ i = \sqrt{\dfrac{ab^3 - a_1b_1^3}{12(ab - a_1b_1)}} \end{cases} \tag{5}$$

where a and b are the length and width of the cross section, respectively; a_1 and b_1 are the internal length and width of

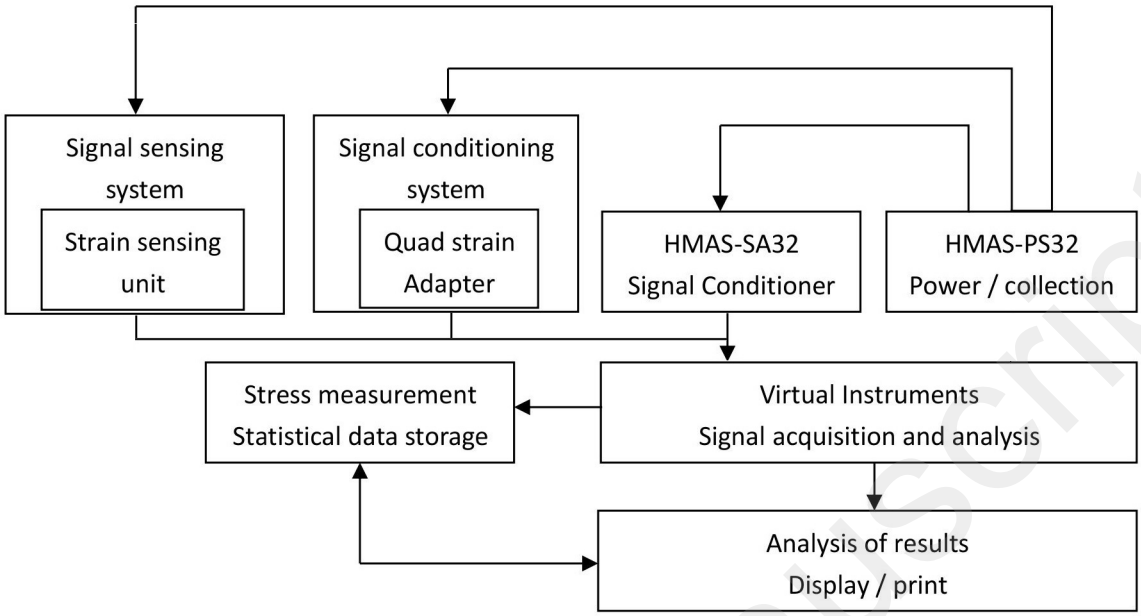

FIGURE 1. Testing system.

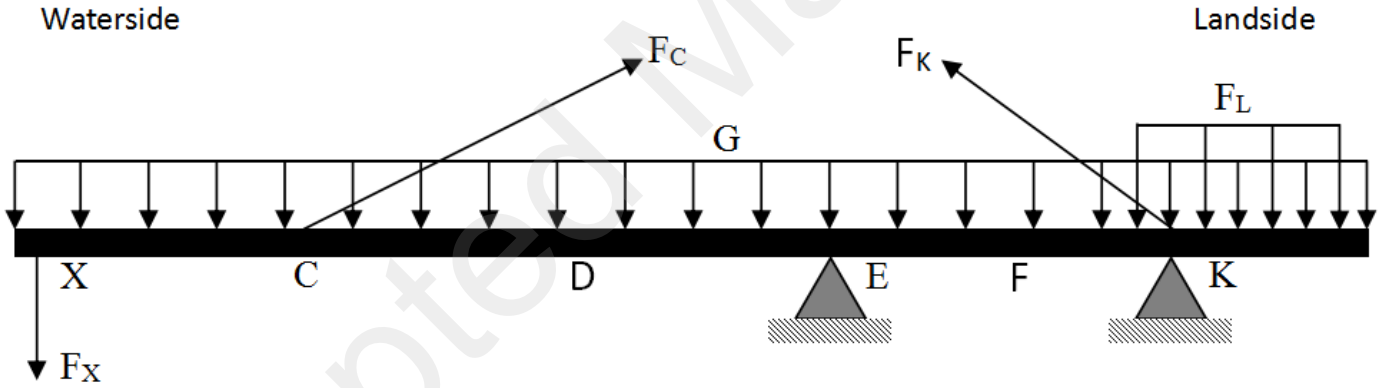

FIGURE 2. Reaction for the beam.

F_X : Dynamic load (Self-weight of trolley and hopper, and test load); F_C : Force of the diagonal link reaction on point C; F_L : Weight of the house (Machinery house, electric room, power station and so on); G : Self-weight of the beam; D : Center between C and E; F : Center between E and K. F_K : Force of the diagonal link reaction on point K.

the cross section, respectively; e is the extreme point; and i is the radius of gyration [15].

By calculating σ, we find that the maximum σ must appear at points C, D, E, F, or K (as shown in Figure 2). These sensors will be placed at these positions. Theoretically, the diagonal link connects with the beam at point C. However, in practice, the diagonal link connects with the beam at points A and B by lugs, so the sensors are set at the points A and B instead of point C. All of the measurement points are shown in Figure 4. To reduce the number of sensors to 14, U_1, U_3, U_5, and U_7 (see Figure 4) are considered to have the same mechanical properties. Similarly, D_1, D_3, D_5, and D_7 are considered the same. The same applies to M_1 and M_5, and M_2 and M_6. Therefore U_5 and D_7 are chosen as measurement points at A, B, D, and F; and M_1 and M_6 are chosen as measurement points at E and K. In addition, U_3 and U_7 are measured at point D to improve measurement accuracy. These points have been labeled AU5, AD7, BU5, BD7, DU5, DU7, DD7, DU3, EM1, EM6, FU5, FD7, KM1, and KM6.

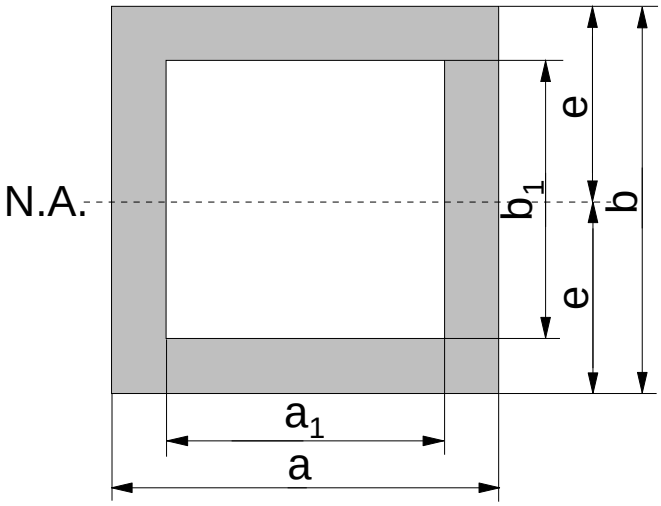

FIGURE 3. Cross section of the beam (view from waterside to landside).

C. LOADING AND CONDITION

Main structure testing with dynamic load stress is based on a static stress test. With static stress tests, including quantitative distributions and static load waveforms [16], we can analyze the features of large static stress points in both amplitude and frequency domains, and then check the strength of the structure with a dynamic load.

The positions with different loading and conditions are shown in Figure 5. The test load is 25 tons (nominal load of 28 tons). The wind scale was 3 and the environmental temperature was 25°C. We have conducted a total of 10 cyclic experiments from testing condition 0 to testing condition 4, and calculated the average cycle time, which was 200 s. The on-site test conditions (TC - Testing Condition) are:

1) TC0 (from position 0 to position 1): In this zero state condition, the test load is located in the hopper, and the grab bucket rests on the test load. The rope is loosened until there is no force between the trolley and the grab bucket.
2) TC1 (from position 1 to position 2): First, the trolley runs at full speed to the limit position of the front beam and the grab bucket begins to free fall. Then, the control wire rope makes the bucket stop for 10 seconds, after which the bucket grabs the test load, and it begins to rise at full speed. Finally, the control wire rope makes the grab bucket stop.
3) TC2 (from position 2 to position 3): First, the trolley runs to the middle position of the front beam and the grab bucket begins to free fall with the test load. Then, the control wire rope makes the bucket stop for 10 seconds, after which it begins to rise at full speed. Finally, the control wire rope makes the grab bucket stop.
4) TC3 (from position 3 to position 4): First, the trolley runs to the position of the back beam and the grab bucket begins free fall with the test load. Then, the control wire rope makes the bucket stop for 10 seconds, after which it begins to rise at full speed. Finally, the control wire rope makes the grab bucket stop.
5) TC4 (from position 4 to position 0): The trolley runs back to the zero position of the beam. The grab bucket lays down the test load. The system goes back to zero and checks the zero drift of the test system.

III. RESULTS AND ANALYSIS

A. DATA COLLECTION

As described previously, data are collected from 14 sensitive points at varying positions along the beam and around the beam cross-section.

B. KALMAN FILTERING

The sampling rate of the signal voltages is 2500Hz. However, the field environment is complex, causing noise that interferes with the signal. To improve the efficiency of data analysis, it is necessary to process the data with a Kalman filter. The general linear discrete system can be expressed as

$$\begin{cases} X(k) = A(k)X(k-1) + B(k)U(k) + w(k) \\ Z(k) = H(k)X(k) + v(k) \end{cases} \tag{6}$$

where $X(k)$ is the n-dimensional state vector; $U(k)$ is the system control vector; $w(k)$ is the n-dimensional system noise vector; $A(k)$ is the state transition matrix from $k-1$ to k; $B(k)$ is the excitation transfer matrix from $k-1$ to k; $Z(k)$ is the m-dimensional observation vector; $H(k)$ is the predictive output transfer matrix for time k; and $v(k)$ is the m-dimensional observation noise vector [17]. The Kalman filter is applied to data prediction, which requires the use of predictive derivation equations as follows:

$$\begin{cases} X(k|k-1) = A(k)X(k-1|k-1) + B(k)U(k) \\ P(k|k-1) = A(k)P(k-1|k-1)A(k)^T + Q \\ X(k|k) = X(k|k-1) + Kg(k)(Z(k) - H(k)X(k|k-1) \\ Kg(k) = P(k|k-1)H(k)^T/(H(k)P(k|k-1)H(k)^T + R) \\ P(k|k) = (I - Kg(k)H(k)P(k|k-1) \end{cases} \tag{7}$$

where $X(k|k-1)$ is the result of the prediction using the previous state of the system; $X(k-1|k-1)$ is the optimal result of the previous state of the system; $P(k|k-1)$ is the corresponding covariance of $X(k|k-1)$; $P(k-1|k-1)$ is the corresponding covariance of $X(k-1|k-1)$; A^T is the transpose of matrix A; $Q(k)$ is the covariance matrix of $w(k)$; $Kg(k)$ is the Kalman gain at time k; $R(k)$ is the covariance matrix of $v(k)$; and I is the unit matrix [18]. In this system, $x(k)$ represents the system status at time k, and $Z(k)$ represents the pressure measurement at time k, so $n = m = 1$, and the state transition matrix $B(k)$ is a zero matrix. We used Gaussian white noise as our model to better simulate unknown real noise, which is often caused by a combination of many different sources of noise. If we increase the system noise, the Kalman gain will also increase,

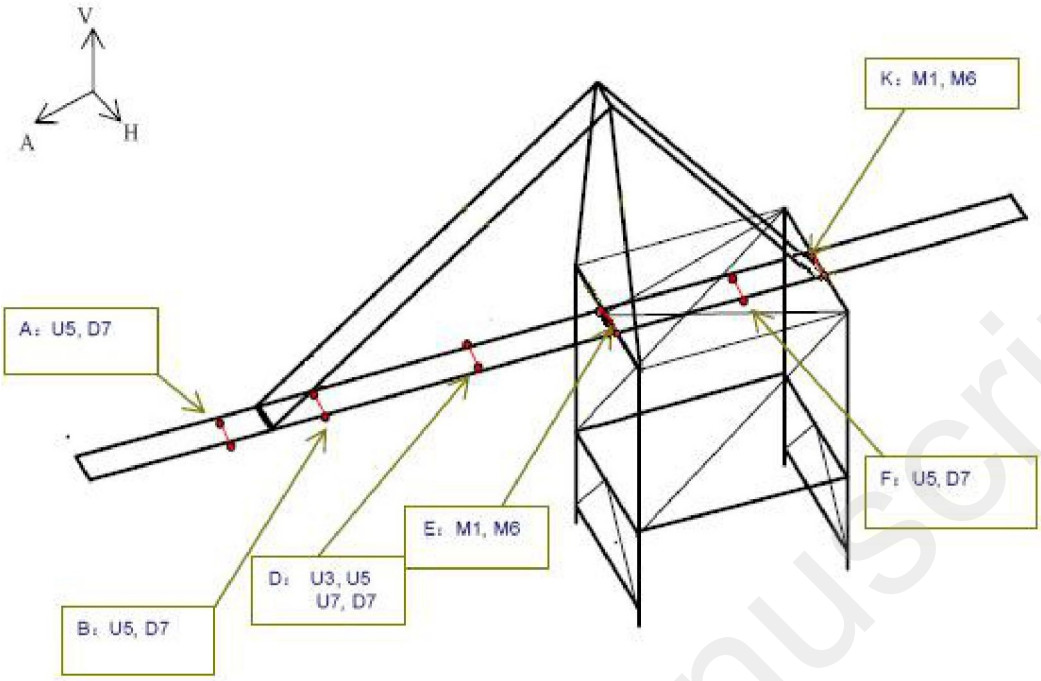

(a)

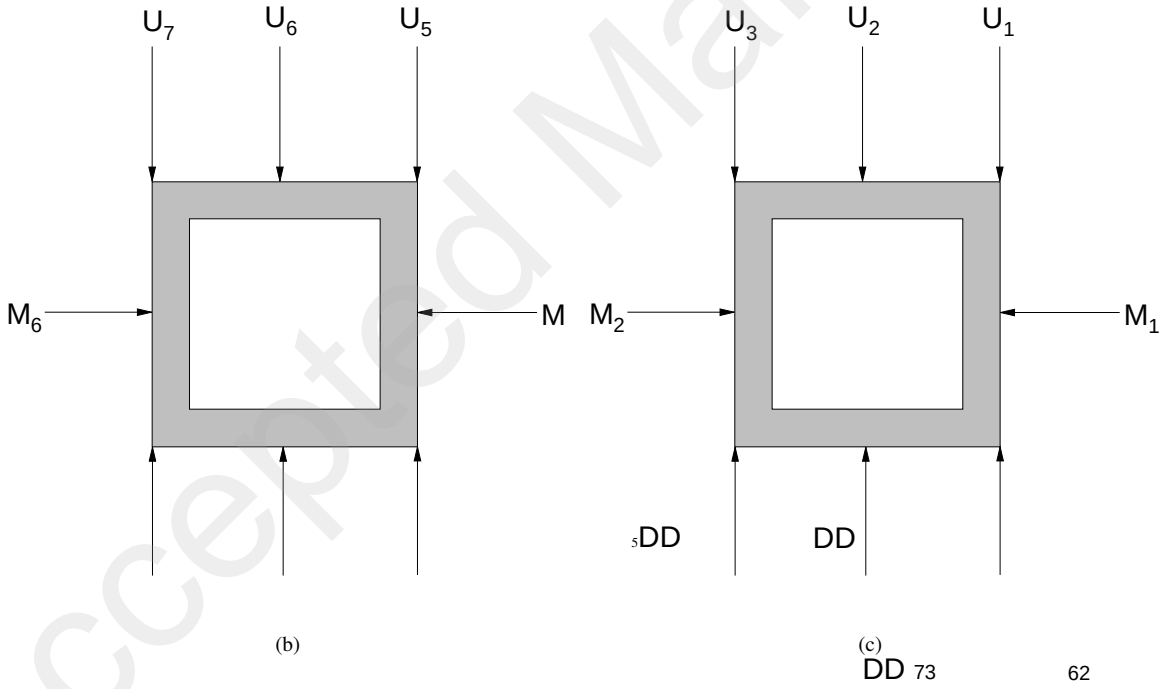

(b) (c)

DD 73 62

FIGURE 4. Positions of the measuring points

Cross sections of left beam and right beam (view from waterside to landside)

making the initial value more reliable; if we increase the measured noise, the Kalman gain will decrease, making the theoretical value become more reliable.

The data processed by Kalman filtering is shown in Figure 6. The horizontal axis is time in seconds, and the vertical axis is stress measured at positions DU3 and DD7 after filtering. We also label the maximum and minimum values after filtering.

C. CALCULATE THE MEASURED POINT STRESS

From the filtered signal, we can obtain the maximum value of stress at each stress measurement point and analyze the corresponding test condition. The calculation results for each measurement point are given in Table 1. The results show that

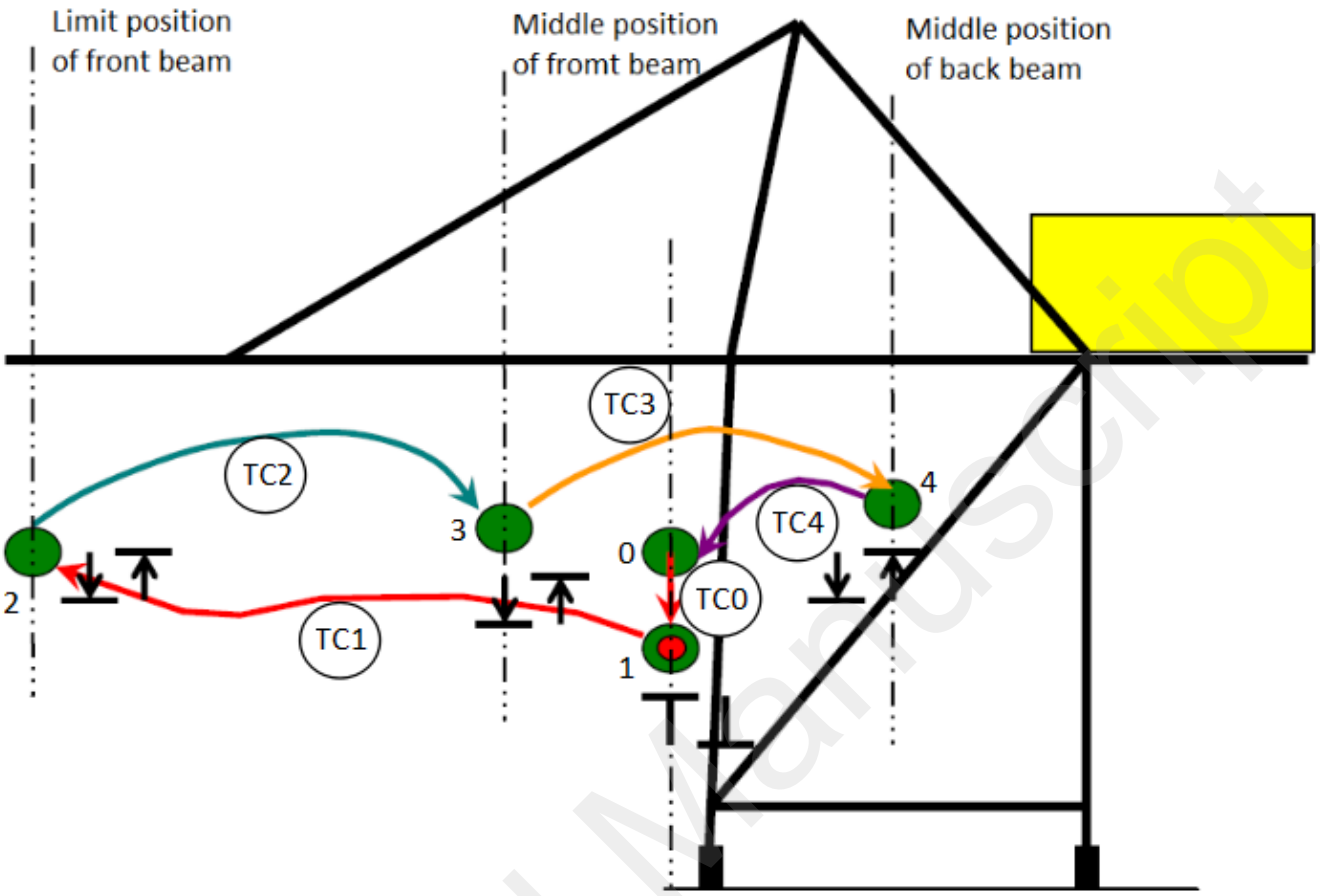

FIGURE 5. Schematic view of the positions with different loading and conditions.

TABLE 1. Structural dynamic load strength (MPa)

Point	Max(MPa)	Time(s)	Min(MPa)	Time(s)
AU5	0	0	-40.09	159
AD7	17.34	41	0	0
BU5	0	0	-40.38	78
BD7	17.16	39	0	0
DU5	0.05	3	-82.60	84
DU7	0.55	2	-82.75	100
DD7	59.90	100	0	0
DU3	1.68	1	-88.49	100
EM1	8.39	91	-0.51	1
EM6	6.10	100	0	0
FU5	36.68	137	-4.40	35
FD7	0.01	4	-19.87	62
KM1	0	0	-4.63	62
KM6	2.67	159	-3.27	62

the maximum compressive stress occurs in condition TC2 (when the trolley runs to the middle position of the front beam), at DU3. The corresponding value is:

$$\sigma_{max}^{(DU3)} = -88.49 \quad (MPa)$$

The maximum tensile stress occurs also in condition TC2, at DD7. The corresponding value is:

$$\sigma_{max}^{(DD7)} = 59.90 \quad (MPa)$$

The STS crane beam is made of steel Q345 (Chinese criterion, similar to S355 in the European criterion, with the same dynamic safety factor), so the allowable stress is given by [15]:

$$[\sigma] = \sigma_y/n = 345/1.5 = 230 \quad (MPa)$$

where σ_y is the yield limit and n is the safety factor for the load. All of the measurement points with dynamic load stress should satisfy the strength requirements:

$$|\sigma|_{max} < [\sigma]$$

In field strength testing, the maximum tensile stress occurs at DD7, with a value of 59.90 MPa; the maximum dynamic load stress occurs at DU3 with a -88.49 MPa. These values meet the strength requirements.

IV. CONCLUSION

This paper introduces a systematic approach to analyzing the strength of the main structural component in an STS crane

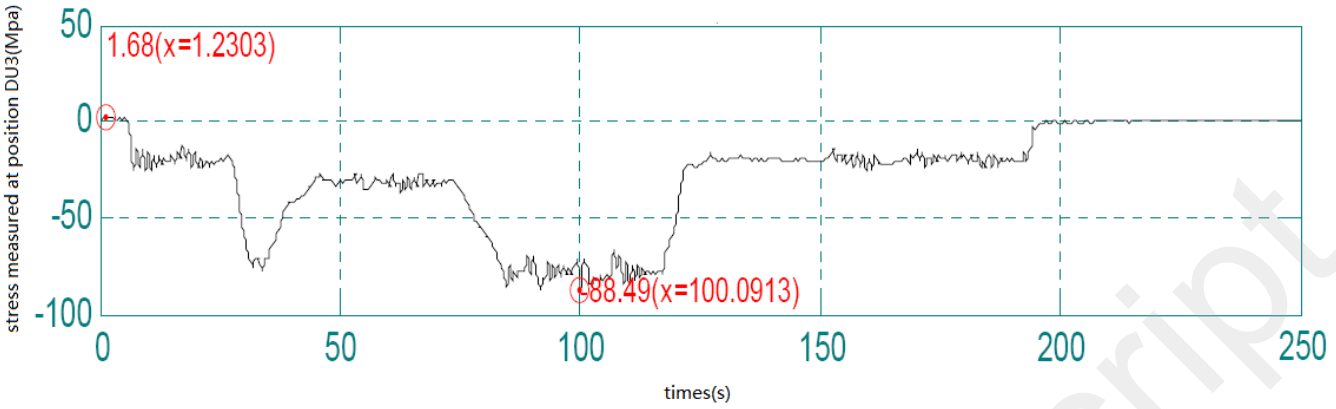

(a)

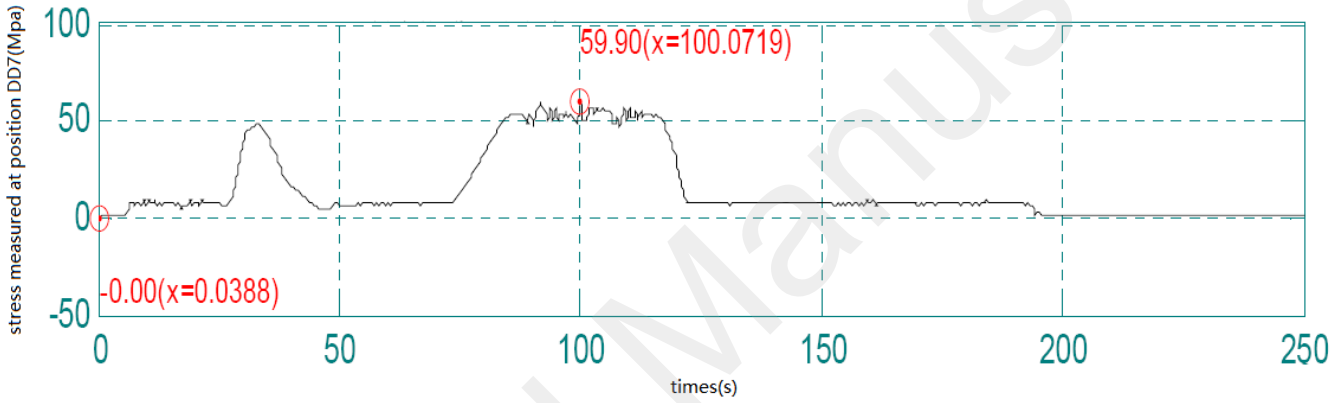

(b)

FIGURE 6. Time-domain curves of stress in maximum stress points

under dynamic load. First, we established a testing system for the main structural component in STS cranes, including signal sensing, conditioning, acquisition, and analysis. Second, we identified dangerous positions at which maximum stress may occur and arranged sensors in these positions. Third, we designed the on-site test conditions, and acquired signals and processed them with Kalman filters. Fourth, we calculated the stresses of the test positions under various test conditions.

However, there are some limitations of our method. Due to safety concerns, we have not conducted field tests under strong wind conditions. When strong winds occur, the structural connections of the crane (such as the connection between the legs and the main beam and the connection between the legs and the lower cross beam) can produce large eddy currents. Large negative pressures will be generated in this zone, creating a strong turbulent flow zone between the two main beams and producing a negative wind pressure.

ACKNOWLEDGMENT

This work was supported by the National Natural Science Foundation of China (No. 31300783), China Postdoctoral Science Foundation (No. 2014M561458), Doctoral Fund of the Ministry of Education Jointly Funded Project (No. 20123121120004), the Shanghai Maritime University Research Project (No. 20130474), the Shanghai Top Academic Discipline Project management science and engineering, and the high-tech research and development program of China (No. 2013A2041106).

REFERENCES

[1] N. Zrnić, D. Oguamanam, and S.Bošnjak, "Dynamics and modelling of mega quayside container cranes," Fme Transactions, vol. 34, no. 4, pp. 193–198, 2006.

[2] U. Nenad Zrni and K. Hoffmann, "Development of design of ship-to-shore container cranes: 1959-2004," 2004.

[3] H. H. Richardson, Static and dynamic load, stress, and deflection cycles in spur-gear systems. PhD thesis, Massachusetts Institute of Technology, 1958.

[4] N. Jones, "Plastic failure of ductile beams loaded dynamically," Journal of Engineering for Industry, vol. 98, no. 1, p. 131, 1976.

[5] J. A. Laman, J. S. Pechar, and T. E. Boothby, "Dynamic load allowance for through-truss bridges," Journal of Bridge Engineering, vol. 4, no. 4, pp. 231–241, 1999.

[6] P. S. Shenoy and A. Fatemi, "Dynamic analysis of loads and stresses in connecting rods," Proceedings of the Institution of Mechanical Engineers – Part C, vol. 220, no. 5, pp. 615–624, 2006.

[7] E. S. Hwang and A. S. Nowak, "Simulation of dynamic load for bridges," Journal of Structural Engineering, vol. 117, no. 5, pp. 1413–1434, 1991.
[8] V. A. Kopnov, "Fatigue life prediction of the metalwork of a travelling gantry crane," Engineering Failure Analysis, vol. 6, no. 3, pp. 131–141, 1999.
[9] G. Hearn and R. B. Testa, "Modal analysis for damage detection in structures," Journal of Structural Engineering, vol. 117, no. 10, pp. 3042–3063, 1991.
[10] Q. Tran, J. Huh, V. Nguyen, C. Kang, J.-H. Ahn, and I.-J. Park, "Sensitivity analysis for ship-to-shore container crane design," Applied Sciences, vol. 8, no. 9, p. 1667, 2018.
[11] Q. Tran, J. Huh, V. Nguyen, A. Haldar, C. Kang, and K. M. Hwang, "Comparative study of nonlinear static and time-history analyses of typical korean sts container cranes," Advances in Civil Engineering, vol. 2018, 2018.
[12] W. Johnson and S. L. Rice, Impact strength of materials. Arnold, 1972.
[13] M. F. Spotts, T. E. Shoup, and L. E. Hornberger, Design of Machine Elements, 8/E. Prentice-Hall, 1978.
[14] S. W. Lee, J. J. Shim, D. S. Han, G. J. Han, and K. S. Lee, "An experimental analysis of the effect of wind load on the stability of a container crane," Journal of Mechanical Science and Technology, vol. 21, no. 3, pp. 448–454, 2007.
[15] F. B. Seely, "Advanced mechanics of materials," Physics Today, vol. 7, no. 4, pp. 26–27, 1954.
[16] G. Tang, X. Hu, W. Wang, T. H. Tang, C. Claramunt, and C. W. Chen, "Structural strength analysis of ship-to-shore crane," in Applied Mechanics and Materials, vol. 858, pp. 34–37, Trans Tech Publ, 2017.
[17] Z. Wang, optimal state estimation and system identification. northwestern polytechnic university press, 2004.
[18] M. S. Bartlett, "An introduction to stochastic processes with special reference to methods and applications.," Technometrics, vol. 65, no. 260, pp. 690–692, 1978.